



ELSEVIER

Journal of Hydrology 237 (2000) 147–168

Journal  
of  
**Hydrology**

www.elsevier.com/locate/jhydrol

## Geochemical modeling of iron, sulfur, oxygen and carbon in a coastal plain aquifer

C.J. Brown<sup>a,\*</sup>, M.A.A. Schoonen<sup>b,c</sup>, J.L. Candela<sup>d</sup>

<sup>a</sup>US Geological Survey, East Hartford, CT 06108, USA

<sup>b</sup>Department of Geosciences, SUNY - Stony Brook, Stony Brook, NY 11794, USA

<sup>c</sup>Long Island Groundwater Research Institute, SUNY - Stony Brook, Stony Brook, NY 11794, USA

<sup>d</sup>US Geological Survey, Coram, NY 11727, USA

Received 6 July 1999; revised 3 May 2000; accepted 13 July 2000

### Abstract

Fe(III) reduction in the Magothy aquifer of Long Island, NY, results in high dissolved-iron concentrations that degrade water quality. Geochemical modeling was used to constrain iron-related geochemical processes and redox zonation along a flow path. The observed increase in dissolved inorganic carbon is consistent with the oxidation of sedimentary organic matter coupled to the reduction of O<sub>2</sub> and SO<sub>4</sub><sup>2-</sup> in the aerobic zone, and to the reduction of SO<sub>4</sub><sup>2-</sup> in the anaerobic zone; estimated rates of CO<sub>2</sub> production through reduction of Fe(III) were relatively minor by comparison. The rates of CO<sub>2</sub> production calculated from dissolved inorganic carbon mass transfer ( $2.55 \times 10^{-4}$  to  $48.6 \times 10^{-4}$  mmol l<sup>-1</sup> yr<sup>-1</sup>) generally were comparable to the calculated rates of CO<sub>2</sub> production by the combined reduction of O<sub>2</sub>, Fe(III) and SO<sub>4</sub><sup>2-</sup> ( $1.31 \times 10^{-4}$  to  $15 \times 10^{-4}$  mmol l<sup>-1</sup> yr<sup>-1</sup>). The overall increase in SO<sub>4</sub><sup>2-</sup> concentrations along the flow path, together with the results of mass-balance calculations, and variations in δ<sup>34</sup>S values along the flow path indicate that SO<sub>4</sub><sup>2-</sup> loss through microbial reduction is exceeded by SO<sub>4</sub><sup>2-</sup> gain through diffusion from sediments and through the oxidation of FeS<sub>2</sub>. Geochemical and microbial data on cores indicate that Fe(III) oxyhydroxide coatings on sediment grains in local, organic carbon- and SO<sub>4</sub><sup>2-</sup>-rich zones have been depleted by microbial reduction and resulted in localized SO<sub>4</sub><sup>2-</sup>-reducing zones in which the formation of iron disulfides decreases dissolved iron concentrations. These localized zones of SO<sub>4</sub><sup>2-</sup> reduction, which are important for assessing zones of low dissolved iron for water-supply development, could be overlooked by aquifer studies that rely only on groundwater data from well-water samples for geochemical modeling. © 2000 Elsevier Science B.V. All rights reserved.

**Keywords:** Geochemistry; Aquifer; Coastal plain; Iron; Sulfur; Groundwater

### 1. Introduction

Sediments in passive-margin basins generally are older (Veizer and Jansen, 1985), and, therefore, more weathered than sediments in other global tectonic settings. Furthermore, redox reactions are

some of the most important chemical processes within nonmarine coastal-plain deposits (Trapp and Meisler, 1992). Concentrations of redox-active constituents such as iron, sulfur, carbon and oxygen in coastal plain aquifers generally are high and are dependent on the distribution of sedimentary organic matter (SOM). Lignitic organic matter can be mineralized by fermentative bacteria to produce organic acids, which subsequently are oxidized to CO<sub>2</sub> by a terminal

\* Corresponding author.

E-mail address: cjbrown@usgs.gov (C.J. Brown).

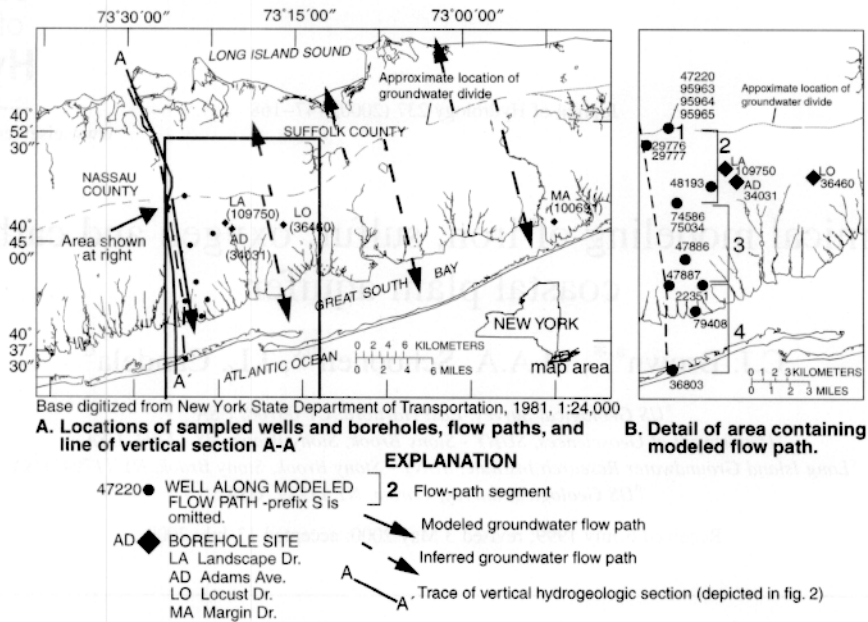


Fig. 1. Pertinent geographic features of study area, Long Island. (Section A-A' depicted in Fig. 2).

electron-accepting process (TEAP) such as microbial Fe(III) reduction,  $\text{SO}_4^{2-}$  reduction, or methanogenesis (Chapelle et al., 1988; McMahon and Chapelle, 1991).

Rates of SOM metabolism generally are high in local, aerobic flow systems and near recharge areas but decrease with increasing distance along flow paths as the supply of dissolved oxygen is consumed; the primary electron acceptors then become Fe(III),  $\text{SO}_4^{2-}$  and  $\text{CO}_2$  (Appelo and Postma, 1993). Many unconsolidated aquifers do not conform to this sequential ordering of TEAPs, however, because their distribution of SOM and Fe(III) coatings in sediments, and  $\text{SO}_4^{2-}$  concentrations in water, is irregular (Chapelle et al., 1995). For example, aerobic parts of the Midden-dorf aquifer of South Carolina contain anaerobic microenvironments, within and surrounding organic matter, that mainly support  $\text{SO}_4^{2-}$  and (or) Fe(III) reduction (Murphy et al., 1992). In addition, several researchers have used pore-water chemistry data together with well-water data from coastal-plain aquifers to show that poorly permeable sediments are a principal source of  $\text{SO}_4^{2-}$  for microbially induced  $\text{SO}_4^{2-}$  reduction (e.g. Chapelle et al., 1987; McMahon et al., 1990; Pucci et al., 1992). However, many geochemical-modeling studies of aquifers rely solely

on data from wells and, thus, can overlook localized processes that affect the biogeochemistry of the aquifer system.

Dissolved iron is a major concern for water suppliers on Long Island, NY (Walter, 1997); therefore, data on iron sources and sinks, and the effects of TEAP zones on iron concentrations within the Magothy aquifer, are needed for sound decisions on water management and well siting. In 1994, the US Geological Survey, in cooperation with Suffolk County Water Authority, began study of the sources and fate of iron in the aquifer system in terms of the microbial and geochemical cycles of sulfur, carbon and oxygen, which are closely related to the iron cycle. An earlier paper (Brown et al., 1999) describes the geochemistry of localized  $\text{SO}_4^{2-}$ -reducing zones in Magothy sediments as interpreted from analysis of drill-core and pore-water samples from four sites in Suffolk County, and from study of groundwater chemistry along a flow path along the western boundary of Suffolk County. The abundance of Fe(III) oxyhydroxide coatings in the Magothy aquifer of Long Island was found to be low in relation to that in other Atlantic Coastal Plain aquifers, but Fe(III) reduction is active as indicated by TEAP identification of cores amended with ( $^{14}\text{C}$ )-acetate and by isolation of an

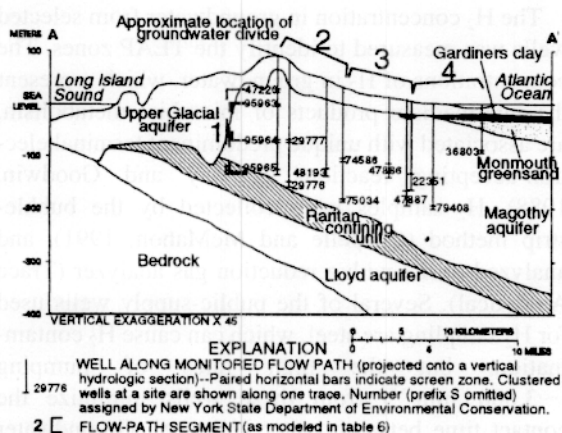


Fig. 2. Hydrogeologic section A-A'. [Modified from Smolensky et al., 1989, sheet 1.]

Fe(III)-reducing organism, MD612. The large spatial variation in concentrations of carbon and iron, which includes the depletion of Fe(III) oxyhydroxide coatings by microbial reduction in organic carbon- and  $\text{SO}_4^{2-}$ -rich zones, has resulted in localized  $\text{SO}_4^{2-}$ -reducing zones in which the formation of  $\text{FeS}_2$  lowers dissolved iron concentrations (Brown et al., 1999). Because of the large spatial variation in carbon, iron, sulfur and TEAPs within the aquifer, further study of the biogeochemical cycles of carbon, iron and sulfur, and their interaction was necessary to understand the sources and sinks of iron.

This paper uses microbial and geochemical data from four boreholes and wells in Suffolk County (Brown et al., 1999) together with new data on sediment coatings, pore-water chemistry,  $\delta^{34}\text{S}$  and  $\delta^{13}\text{C}$  of groundwater and solid phases, and  $\text{H}_2$  concentrations in groundwater, to describe the effects of aquifer mineralogy, TEAPs, and mass transfer on the distribution of oxygen, iron, sulfur, carbon along a deep flow path in the Magothy aquifer. Data collected on both a localized scale (0.1–10 m) and at a large scale (10–20,000 m) were required to define overall microbial and geochemical processes and for mass-transfer modeling of  $\text{CO}_2$  production rates by the reduction of  $\text{O}_2$ , Fe(III) and  $\text{SO}_4^{2-}$ .

## 2. Hydrogeologic setting

Long Island consists of a sequence of upper

Cretaceous and Pleistocene sediments that were deposited on a southeastward dipping bedrock surface (Figs. 1 and 2). The deposits thicken southeastward and reach a maximum thickness of over 600 m in southeastern Long Island. Bedrock is overlain by the Lloyd Sand Member (Lloyd aquifer) and the clay member of the Raritan Formation (Raritan confining unit). The Raritan is overlain by the Matawan Group and Magothy Formation, undifferentiated, which comprise the principal aquifer (Magothy), of Cretaceous age. Along the southern shore, the Magothy aquifer is unconformably overlain by the Monmouth Group (Monmouth greensand) of Cretaceous age; elsewhere in the southern part of the island, Cretaceous deposits are unconformably overlain by the upper glacial aquifer (Smolensky et al., 1989).

The Magothy aquifer (the focus of this study) consists of alternating beds and lenses of clay, silt, sand and some gravel, as well as some mixtures of these materials (Perlmutter and Geraghty, 1963). The Magothy was deposited in a transitional fluviodeltaic environment (Lonnie, 1982). The sand consists mostly of quartz but contains some lignite, muscovite and iron concretions and is about 2–3% heavy minerals by weight; it generally has no carbonate minerals and few other reactive minerals, although organic carbon in the form of lignite is a reactive electron donor in redox reactions (Pearson and Friedman, 1970). Lignite is typically found in silts and clays but may be dispersed through the sand (Smolensky et al., 1989). Much of the iron in the Magothy aquifer on Long Island is in the form of Fe(III) oxyhydroxides, iron-sulfide minerals ( $\text{FeS}_2$ ), iron-rich clay minerals and other less soluble minerals, including hematite, leucoxene, ilmenite and magnetite (Brown et al., 2000). The clays consist mostly of kaolinite, some illite, and occasional traces of mixed-layer clays; iron is less abundant in Magothy clays than in marine clays (Lonnie, 1982).

The Long Island groundwater system is recharged solely by precipitation. Most of the recharge enters the water table, moves laterally through the upper glacial aquifer and discharges to streams or to coastal waters. Precipitation near the mid-island groundwater divide (Fig. 1) flows downward and recharges the Magothy and Lloyd aquifers after passing a short distance through the upper glacial aquifer (in most areas), and then flows to either the north or south shore.

Buxton and Modica (1992) concluded that Magothy water beneath the south shore is several hundred years old on the basis of a sectional finite-element model that was used to calculate groundwater travel time along the Nassau–Suffolk border.

Water in the Magothy aquifer has low ionic strength and  $\text{Na}^+$  and  $\text{Cl}^-$  are the dominant ions. The  $\text{K}^+/\text{H}^+$  and  $\text{Na}^+/\text{H}^+$  ratios and silica content (Pearson and Friedman, 1970), and an analysis of clay mineralogy (Lonnie, 1982; B. Sirois, unpublished data, 1986), indicate that Magothy water is in equilibrium with kaolinite. Dissolved oxygen concentrations in the Magothy aquifer are as high as  $0.28 \text{ mmol l}^{-1}$  near the groundwater divide (recharge area) but decrease to concentrations below detection along the flow path. Dissolved iron concentrations commonly exceed  $9 \mu\text{mol l}^{-1}$  near the south shore, where they contribute to encrustation on well screens (Walter, 1997) and degradation of water quality.

### 3. Methods

Groundwater chemistry was studied in well water along a flow path near the Nassau–Suffolk County border (Fig. 1). Four Suffolk County Water Authority (SCWA) borehole sites were selected for study (Fig. 1); although the boreholes are not along the same flow path, each site represents a different lithology and/or position from the ground-water divide and are used here to evaluate the heterogeneity of the aquifer. The borehole sites were at supply well fields and were subsequently used for installation of public-supply wells.

#### 3.1. Groundwater sampling

Water samples were collected from monitoring wells and public-supply wells screened along the deep modeled flow path (Fig. 1) and at inferred flow paths at each of the four borehole locations. Water-chemistry data were collected by standard procedures (Brown et al., 1970). Colorimetric procedures (Hach Company, 1993) were used onsite to measure concentrations of total dissolved sulfide ( $\text{H}_2\text{S}$  and  $\text{HS}^-$ ), Fe(II) and Fe(III) and dissolved oxygen; a dissolved oxygen meter and the revised Winkler method were used to measure the dissolved oxygen concentrations above  $0.025 \text{ mmol l}^{-1}$ .

The  $\text{H}_2$  concentration in groundwater from selected wells was measured to identify the TEAP zones. The concentrations of  $\text{H}_2$  in groundwater, which represent the intermediate products of microbial metabolism, are associated with unique predominant terminal electron-accepting reactions (Lovley and Goodwin, 1988).  $\text{H}_2$  samples were collected by the bubble-strip method (Chapelle and McMahon, 1991), and analyzed onsite with a reduction gas analyzer (Trace Analytical). Several of the public-supply wells used for  $\text{H}_2$  sampling are steel, which can cause  $\text{H}_2$  contamination, but the high rates of pumping ( $\sim 3,800 \text{ l min}^{-1}$ ) from these wells minimize the contact time between water and steel. Groundwater  $\text{SO}_4^{2-}$  was collected on an anion-exchange resin column for sulfur-isotope analysis and was analyzed for  $\text{BaSO}_4$  precipitates by procedures described in Carmody et al. (1998). Water samples for  $\delta^{13}\text{C}$  analysis of dissolved inorganic carbon (DIC) were collected in 1-l glass bottles, which were filled from the bottom up and sealed with a Teflon/silicon septa cap after a minimum of 3–5 l were allowed to overflow to eliminate oxygen.

#### 3.2. Drilling and sediment sampling

Split-spoon cores (3.8 cm diameter) were obtained from sediments of the Magothy aquifer at the four SCWA borehole sites (Fig. 1) by a reverse-rotary drill rig. Several cores from each borehole site were selected for analysis — five (AD1–AD5) from Adams Ave., three (LA1–LA3) from Landscape Dr., six (LO1–LO6) from Locust Dr. and four (MA1–MA4) from Margin Dr. Detailed sediment lithology and microbiology of these boreholes and the procedure for the collection of core samples, which were subsampled under a stream of  $\text{N}_2$ , are described in Brown et al. (1999). Core samples generally yielded insufficient pore water for analysis; therefore, 30–50 g of subsampled core were mixed with 2–10 ml deionized water for 1–3 min, and followed by filter pressing with  $\text{N}_2$  (Luszczynski, 1961) as described in Brown et al. (1999).

#### 3.3. Laboratory analyses

Alkalinity of water samples was measured by incremental titration within a few hours after sample collection. Concentrations of major and minor

Table 1

Concentration of iron and manganese in sediment-coating extractions of core samples from the four boreholes, Suffolk County, NY (site locations shown in Fig. 1. Concentrations in micromoles per gram of sediment. Altitudes in meters from sea level. – data not available)

Sample No.	Sample altitude	Speciation and extraction method <sup>a</sup>					
		Fe (total) 0.5 M HCl <sup>b</sup>	Fe (II) 0.5 M HCl <sup>c</sup>	Fe (III) 0.5 M HCl <sup>d</sup>	Ion-exchangeable Fe(II) <sup>e</sup>	Fe (total) 5 M HCl <sup>f</sup>	Mn (total) 5 M HCl <sup>f</sup>
<i>A. Adams Ave. (AD), land-surface altitude 18.48 m</i>							
AD 1	-119	<0.1	<0.1	<0.1	0.22	5.7	<0.1
AD 2	-125	<0.1	<0.1	<0.1	<0.1	9.9	<0.1
AD 3	-131	0.28	<0.1	0.21	0.11	3.6	0.16
AD 4	-134	0.82	0.74	<0.1	<0.1	9.1	0.34
AD 5	-137	0.89	0.60	0.30	<0.1	11	0.11
<i>B. Landscape Dr. (LA), land-surface altitude 54.36 m</i>							
LA 1	-147	<0.1	<0.1	<0.1	1.0	49	0.43
LA 2	-174	1.1	0.79	0.32	1.2	9	<0.1
LA 3a	-177a	<0.1	<0.1	<0.1	0.23	9.2	<0.1
LA 3b	-177b	1.2	0.49	0.69	–	13	<0.1
<i>C. Locust Dr. (LO), land-surface altitude 23.2 m</i>							
LO1a	-124	2.6	1.3	0.19	0.11	–	–
LO 1	-145	2.5	0.93	1.3	0.39	11	>0.1
LO 2	-148	0.93	0.84	1.6	0.45	4.1	0.11
LO 3	-152	1.2	0.98	0.09	0.37	5.5	0.15
LO 4	-158	0.75	0.68	0.07	0.47	3.5	0.12
<i>D. Margin Dr. (MA), land-surface altitude 7.62 m</i>							
MA 1	-142	4.3	4.0	0.28	4.1	49	0.13
MA 2	-173	0.50	0.27	0.24	0.97	33	0.46
MA 3	-176	1.0	0.77	0.28	0.28	28	0.31
MA 4	-179	0.14	0.10	<0.1	0.14	8	<0.1

<sup>a</sup> Values are the means of five replicates.

<sup>b</sup> Measured after extraction with 6.25 M hydroxylamine in 0.5 M HCl (from Brown et al., 1999).

<sup>c</sup> Measured after extraction with 0.5 M HCl (from Brown et al., 1999).

<sup>d</sup> Calculated as Fe (total) minus Fe(II) (from Brown et al., 1999).

<sup>e</sup> Measured after extraction with 1 M CaCl<sub>2</sub>·0.

<sup>f</sup> Measured after extraction with 6.25 M hydroxylamine in 5 M HCl.

Table 2

Abundances of carbon and total sulfur in core sediments from the four borehole sites (locations shown in Fig. 1. Altitudes in meters from sea level)

Sample No.	Sample altitude	Sedimentary organic carbon (wt %)	Sedimentary carbonate carbon (wt %)	Total sulfur (wt %)
<i>A. Adams Ave. (AD), land-surface altitude 18.48 m</i>				
AD 1	-119	0.61	<0.01	<0.01
AD 2	-125	0.10	<0.01	0.07
AD 3	-131	<0.01	<0.01	<0.01
AD 4	-134	0.10	<0.01	<0.01
AD 5	-137	0.27	<0.01	0.33
<i>B. Landscape Dr. (LA), land-surface altitude 54.36 m</i>				
LA 1	-147	8.04	<0.01	0.19
LA 2	-174	<0.01	<0.01	<0.01
LA 3	-177	<0.01	<0.01	<0.01
<i>C. Locust Dr. (LO), land-surface altitude 23.2 m</i>				
LO 1	-145	4.51	<0.01	0.28
LO 2	-148	0.09	<0.01	<0.01
LO 3	-152	0.40	<0.01	0.05
LO 4	-158	0.05	<0.01	<0.01
<i>D. Margin Dr. (MA), land-surface altitude 7.62 m</i>				
MA 1	-142	13.9	0.01	2.05
MA 2	-173	1.46	<0.01	0.63
MA 3	-176	0.27	<0.01	0.11
MA 4	-179	0.33	<0.01	0.19

dissolved ions were analyzed by ICP and ion chromatography. Sulfur-isotopic analyses of water and iron disulfide samples were conducted at the USGS Geochemistry Laboratory in Reston, Va.; results are reported (in ‰) relative to the Vienna Canyon Diablo Troilite (VCDT) standard. Carbon isotope analysis of water samples and lignite samples were conducted at the University of Waterloo, in Waterloo, Canada, and are reported (in ‰) relative to the Vienna Peedee Belemnite (VPDB) standard. The uncertainty associated with  $\delta^{34}\text{S}$  and  $\delta^{13}\text{C}$  values is  $\pm 0.2\%$ . Geochemical mass-balance modeling with NETPATH was used to help estimate mass-transfer rates.

The abundance of various types of iron coatings was evaluated in the samples taken. Iron coatings on sediments were identified through 5 M HCl extraction (Heron et al., 1994b) for comparison with 0.5 M HCl-hydroxylamine-extractable iron (Lovley and Phillips, 1987) measured by Brown et al. (1999). The amount of Fe(II) soluble in 1 M  $\text{CaCl}_2$  at pH 7.0, which yields ion-exchangeable Fe(II), was measured by an

anaerobic 24-h extraction at 20°C followed by colorimetric analysis of dissolved Fe(II) (Heron et al., 1994a).

Iron-sulfide minerals were hand separated from bulk samples, ground to a powder, and identified as either pyrite or marcasite by powder X-ray diffraction (Scintag). Scanning electron microscopy (SEM) and reflected light microscopy were used to define crystal morphology of the selected samples.

#### 4. Results and discussion

Results are presented in two sections — aquifer geochemistry, which discusses lithology, water quality, and chemical reactions, and mass-transfer modeling, which discusses mass-transfer rates of carbon, oxygen, iron and sulfur.

##### 4.1. Aquifer geochemistry

Concentrations of 5 M HCl extractable iron (total) coatings ( $3.5\text{--}49\ \mu\text{M g}^{-1}$  of sediment) and

Table 3

Concentrations of major constituents and pH in pore-water samples from two of the four borehole sites, Suffolk County, NY (concentrations in millimoles per liter. Altitudes in meters from sea level. Site locations shown in Fig. 1)

Borehole location	Core altitude	pH	Fe, dissolved	Ca <sup>2+</sup>	Mg <sup>2+</sup>	Na <sup>+</sup>	SO <sub>4</sub> <sup>2-</sup>	Cl <sup>-</sup>	Br <sup>-</sup>	Silica
<i>Landscape Dr. (LA)</i>										
LA1	-146.9	4.73	0.0180	0.014	0.012	0.267	0.154	0.168	0.002	0.388
LA2	-174.3	5.32	0.0050	0.154	0.085	0.472	0.668	1.15	0.011	0.378
LA3	-177.4	5.05	0.0090	0.261	0.146	0.527	0.281	0.482	0.004	0.428
<i>Margin Dr. (MA)</i>										
MA1	-142.4	5.06	0.0010	0.009	0.0217	0.174	0.420	0.693	0.005	0.064
MA2	-172.9	6.24	0.0002	0.038	0.0462	0.274	0.343	0.500	0.0045	0.203
MA3	-175.9	4.39	0.0034	0.168	0.214	0.315	0.405	1.52	0.0027	0.151
MA4	-179.0	7.22	0.0027	0.022	0.027	1.81	0.953	0.690	0.0048	0.275

ion-exchangeable Fe(II) (<0.1–4.1  $\mu\text{M g}^{-1}$  of sediment) are low (Table 1) and relatively consistent with the low concentrations of 0.5 M HCl extractable iron coatings (<0.1–4.3  $\mu\text{M g}^{-1}$ ) measured by Brown et al. (1999). The 5 M HCl extractable iron (total) indicates the amounts of both crystalline and poorly crystalline iron coating and generally was at least an order of magnitude greater than the 0.5 M HCl extractable iron (Table 1). The 0.5 M HCl extraction indicates the amount of poorly crystalline Fe(III) in the sample and also, presumably, the most microbially reactive iron fraction. Concentrations of 5 M HCl extractable manganese (total) coatings (<0.1–0.46  $\mu\text{M g}^{-1}$  of sediment) generally were 1–2 orders of magnitude lower than the 5 M HCl extractable iron (total) coatings (Table 1), and consistent with relative concentrations of dissolved iron and manganese in groundwater.

Percentages of organic carbon and total sulfur differ widely among the four sites (Table 2) and are consistent with these data from a borehole in western Suffolk County (Brown et al., 2000). The uneven distribution of Fe(III) concentrations, carbon and total sulfur in Magothy aquifer sediments indicates that localized microenvironments are prevalent throughout the Magothy aquifer.

#### 4.1.1. Well-water and pore-water chemistry

Concentrations of pore-water constituents (Table 3) were significantly higher than in water (Table 4) from nearby wells screened in the Magothy aquifer (Brown et al., 1999), but were much lower than in seawater. Pore-water samples from a short interval, particularly

in poorly permeable sediments, were likely to be more representative of a single lithology than were groundwater samples (from wells screened over distances of 5–27 m), which reflect a far greater thickness of sediment. Concentrations of major ions in pore-water samples were from 10 to 100 times greater than those in groundwater samples and can result in localized microbial and geochemical reactions that are not apparent in large-scale aquifer studies based solely on well-water analyses.

Dissolved-oxygen concentrations in the Magothy aquifer can be high (up to 0.34 mmol l<sup>-1</sup>) near the groundwater divide of western Suffolk County but decrease with distance along the deep flow path (Fig. 3A), whereas dissolved iron concentrations are low near the divide and increase with distance (Fig. 3B). Sulfate concentrations also increase downgradient (Fig. 3C), despite the predominance of SO<sub>4</sub><sup>2-</sup>-reducing TEAPs along much of the flow path. The concentrations of dissolved inorganic carbon (DIC) (Fig. 3D) and pH also increase along the flow path.

The low ionic strength of Magothy waters, coupled with the saturation of the aquifer sediment with sea water during sediment deposition or during later seawater transgression (Brown, 1998), has resulted in a chemical gradient where sorbed constituents such as SO<sub>4</sub><sup>2-</sup> represent an in situ ion source. A study of anion exchange on Magothy sediments (Brown, 1998) shows that in areas of low pH or high-ionic-strength water, significant amounts of Cl<sup>-</sup> and SO<sub>4</sub><sup>2-</sup> (3.7–20  $\mu\text{g g}^{-1}$  and 44–130  $\mu\text{g g}^{-1}$  of sediment, respectively) can be sorbed in fine-grained sediments in the Magothy aquifer, particularly those with high

**Table 4**  
 Concentrations of major elements, chemical species,  $\delta^{13}\text{C}$ , and  $\delta^{34}\text{S}$ , in water samples from selected wells, Suffolk County, NY, sampled from 1995–1997 (dissolved concentrations in millimoles per liter. Screen interval in meters from sea level. – data not available. Locations shown in Fig. 1)

Well site	Screen interval	pH	O <sub>2</sub>	Ca <sup>2+</sup>	Mg <sup>2+</sup>	Na <sup>+</sup>	K <sup>+</sup>	HCO <sub>3</sub> <sup>-</sup>	H <sub>2</sub> S	SO <sub>4</sub> <sup>2-</sup>	Cl <sup>-</sup>	Silica	NO <sub>3</sub> <sup>-</sup> as N	Fe	Mn	DOC	$\delta^{13}\text{C}$	$\delta^{34}\text{S}$	
S47220	26.3–29.4	11.8	0.8	0.34	0.0039	0.0017	0.12	0.010	0.040	–	0.0042	0.12	0.088	0.0036	0.0020	0.00040	0.050	-21.4	13.2
S95963	-3.1 to -6.2	12.9	4.99	0.29	0.032	0.045	0.19	0.021	0.054	–	0.0028	0.19	0.12	0.16	0.00022	0.00011	0.017	–	8.8
S95964	-68.9 to -71.9	11.4	0.19	0.22	0.024	0.014	0.13	0.012	0.16	–	0.0022	0.11	0.096	0.020	0.00014	0.00038	0.017	-21.6	6.7
S95965	-133 to -136	11.5	0.00	0.10	0.021	0.014	0.14	0.0077	0.080	<0.0002	0.012	0.12	0.10	0.037	0.035	0.00046	0.017	–	-4.6
S29776	-158 to -161	12.5	0.40	0.066	0.013	0.013	0.095	0.0060	0.20	–	0.018	0.079	0.10	<0.0036	0.0037	0.00020	0.0083	–	-3.6
S29777	-59.2 to -62.2	11.9	0.44	0.11	0.030	0.014	0.17	0.012	0.14	–	0.0094	0.11	0.10	0.093	0.00011	0.00030	<0.0083	–	-7.7
S34031	-122 to -142	11.0	4.92	0.056	0.0087	0.0082	0.14	0.0094	0.040	–	0.022	0.12	0.12	0.0071	0.0017	0.00050	–	-22.2	-3.7
S48193	-121 to -139	10.9	0.40	0.12	0.014	0.0090	0.10	0.0069	0.053	–	0.0094	0.087	0.11	<0.0036	0.0011	–	0.033	–	-6.7
S75034	-184 to -185	12.5	0.89	0.088	0.0095	0.0090	0.11	0.0082	0.12	<0.0002	0.0094	0.082	0.10	0.0036	0.036	0.00062	0.038	-21.1	-8.4
S74586	-106 to -107	12.9	0.10	0.074	0.022	0.013	0.12	0.0076	0.054	–	0.018	0.13	0.11	0.022	0.00014	0.00004	0.033	–	–
S47886	-119 to -143	11.5	4.50	<0.003	0.018	0.016	0.070	0.012	0.020	0.00032	0.041	0.12	0.12	<0.0036	0.0043	0.00009	–	–	-4.7
S47887	-164 to -191	11.3	4.44	0.0034	0.0037	0.0074	0.070	0.0079	0.032	0.00025	0.026	0.10	0.11	<0.0036	0.0056	0.00009	–	–	-4.7
S22351	-137 to -163	11.7	5.35	0.0025	0.035	0.036	0.14	0.013	0.040	0.00073	0.080	0.13	0.14	<0.0036	0.011	0.00027	0.033	-21.0	-1.7
S79408	-202 to -203	12.2	5.43	<0.0003	0.0095	0.014	0.11	0.0077	0.066	<0.0002	0.029	0.10	0.12	<0.0036	0.0053	0.00011	0.017	–	2.7
S36803	-88.1 to -93	13.1	5.67	<0.003	0.0044	0.019	0.27	0.14	0.14	<0.0002	0.064	0.21	0.12	<0.0036	0.020	0.00026	0.042	–	9.8
S36460 <sup>a</sup>	-134 to -162	11.0	5.50	0.0016	0.037	0.030	0.13	0.0094	0.082	0.0020	0.057	0.10	0.15	<0.0036	0.0040	0.00009	–	-21.2	3.9
S10069 <sup>a</sup>	-155 to -162 -166 to -176	15.0	0.26	0.0008	0.090	0.070	0.21	–	0.40	0.00076	0.046	0.13	0.16	<0.0036	0.0042	0.00007	–	-21.2	-13.4

<sup>a</sup> Well is not along southwestern Suffolk County flowpath.

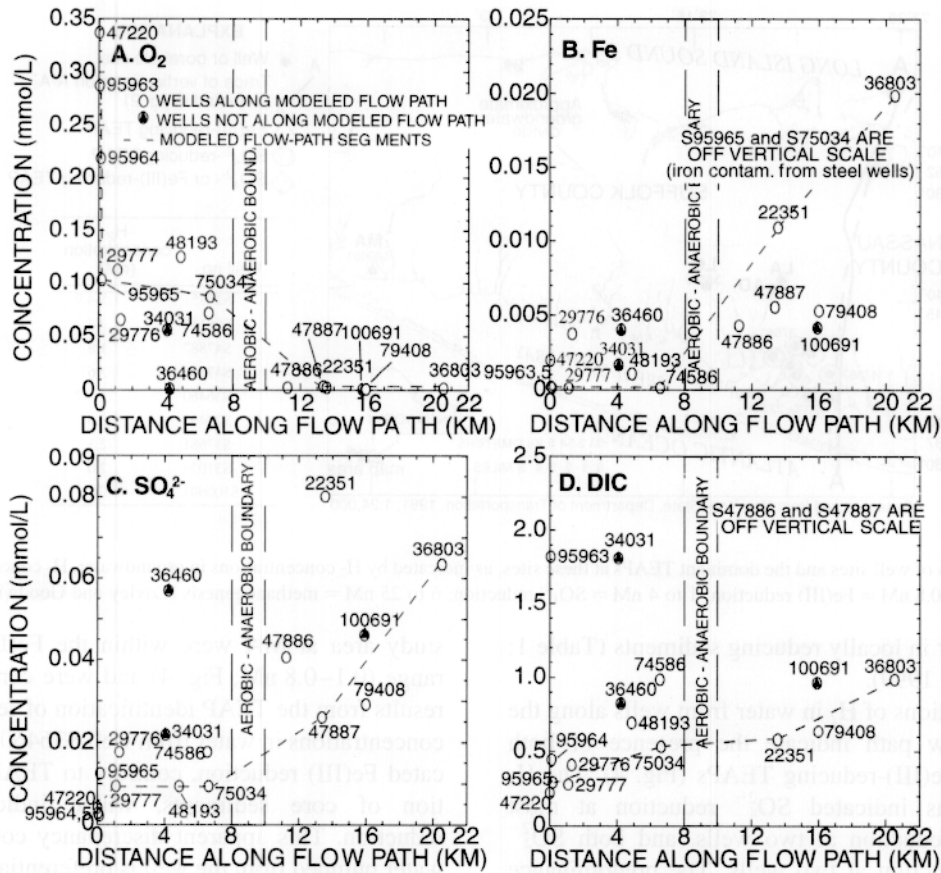


Fig. 3. Concentrations of dissolved (A) oxygen, (B) iron, (C) sulfate, and (D) inorganic carbon, in groundwater along the modeled flow path.

clay and/or SOM content. In addition,  $\text{SO}_4^{2-}$  can be released by oxidation of  $\text{FeS}_2$ , anaerobically, by aqueous Fe(III). The method used for pore-water extraction, therefore, probably resulted in some desorption from sediments, and the results of pore-water analysis (Table 3) probably reflect the desorbed ions in addition to dissolved ions in pore water. Furthermore, some of the measured sulfate may result from oxidation of  $\text{FeS}_2$ .

#### 4.1.2. TEAP distribution

Groundwater along the Magothy flow path (Fig. 1) becomes anaerobic and Fe(III) reducing at 8–10 km south of the groundwater divide, as indicated by the downgradient decrease in dissolved oxygen concentrations (Fig. 3A) and increase in dissolved iron (Fig. 3B) concentrations. Nitrate reduction (denitrification) probably occurs before the reduction of Fe(III), but

the initial nitrate concentrations generally are low because most of the water in the deep-flow system entered before the onset of development in western Suffolk County (Buxton and Modica, 1992). Mn(IV) is reduced after  $\text{NO}_3^-$  and before Fe(III). Although the spatial distribution of manganese concentrations in wells of Suffolk County is similar to that of iron (Walter, 1997), concentrations are lower ( $0.04\text{--}0.62\ \mu\text{mol l}^{-1}$ ) and reflect the lower concentrations in sediment coatings. Dissolved iron represents only a small part of the total iron within an aquifer (Heron and Christensen, 1995) — as much as 98% of the Fe(II) produced by iron reduction is sequestered in sediments in the form of iron-rich clays such as illite, Fe(II)-rich oxides such as magnetite, or sulfides such as pyrite (Chapelle, 1993). The amounts of 0.5 M HCl extractable Fe(II) and ion-exchangeable Fe(II) generally were greater in cores from the anaerobic part of

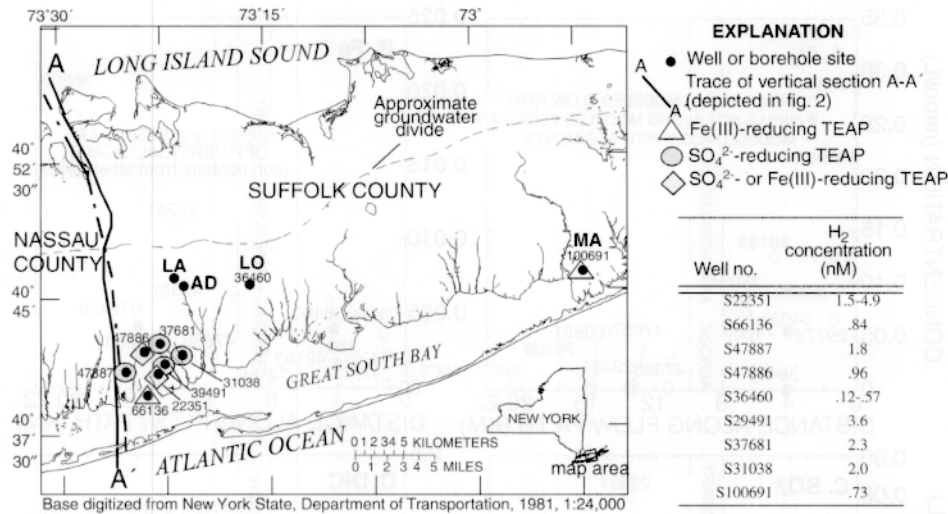


Fig. 4. Locations of well sites and the dominant TEAPs at these sites, as indicated by H<sub>2</sub> concentrations in groundwater. H<sub>2</sub> concentration range for TEAPs: 0.1–0.8 nM = Fe(III) reduction; 1 to 4 nM = SO<sub>4</sub><sup>2-</sup> reduction; 6 to 25 nM = methanogenesis (Lovley and Goodwin, 1988).

the aquifer or in locally reducing sediments (Table 1; Brown et al., 1999).

Concentrations of H<sub>2</sub> in water from wells along the modeled flow path indicate the presence of both SO<sub>4</sub><sup>2-</sup>- and Fe(III)-reducing TEAPs (Fig. 4). The H<sub>2</sub> concentrations indicated SO<sub>4</sub><sup>2-</sup> reduction at most wells, iron reduction at two wells, and both SO<sub>4</sub><sup>2-</sup> and iron reduction at two wells. The predominance of SO<sub>4</sub><sup>2-</sup> reduction, and the local variation in TEAPs and the lack of evidence for their sequential zonation, along the flow path are consistent with the TEAP identification in core samples by (<sup>14</sup>C)-acetate procedures (Brown et al., 1999). Nevertheless, most supply-well screens are more than 15 m in length and can tap several TEAP microenvironments. Microbial analyses of core samples from anaerobic parts of flow paths indicated the presence of both SO<sub>4</sub><sup>2-</sup>- and Fe(III)-reducing bacteria, and analysis of sandy sediments with Fe(III) coatings indicated zones of Fe(III)-reducing TEAPs (Brown et al., 1999). Concentrations of H<sub>2</sub> in groundwater were not indicative of methanogenesis, probably because SO<sub>4</sub><sup>2-</sup> reduction yields greater energy than does the reduction of CO<sub>2</sub> (Lovley and Goodwin, 1988) and SO<sub>4</sub><sup>2-</sup> is abundant in the Magothy. Furthermore, TEAP assays of core sediments showed no evidence of methanogenesis (Brown et al., 1999). H<sub>2</sub> concentrations in water from well S100691 in the southeastern part of the

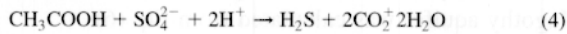
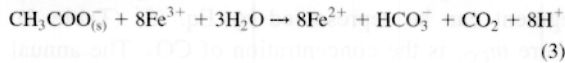
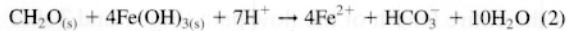
study area at MA were within the Fe(III)-reducing range (0.1–0.8 nM; Fig. 4) and were consistent with results from the TEAP identification of sediments. H<sub>2</sub> concentrations in water from well S36460 at LO, indicated Fe(III) reduction, contrary to TEAP identification of core sediments, which indicated SO<sub>4</sub><sup>2-</sup> reduction. This apparent discrepancy could result if water pumped from the well is preferentially removed from the permeable (sand) sediments, including sediments below the screen, which probably contain Fe(III) reducing TEAPs. Water from the wells at the AD and LA sites (Fig. 4) was not analyzed for H<sub>2</sub> because it contained dissolved oxygen. Supply well S22351, which is in the anaerobic zone near the modeled flow path and is pumped continuously, indicated an alternation between SO<sub>4</sub><sup>2-</sup>- and Fe(III)-reducing TEAPs (Fig. 4) and suggests that water is pumped from different parts of the formation as local hydrologic stresses vary. Although SO<sub>4</sub><sup>2-</sup>-reducing TEAPs predominate in anaerobic parts of the Magothy aquifer, Fe(III)-reducing TEAPs are also present and contribute to the high concentrations of dissolved iron observed (Table 4; Fig. 3B) in water at the downgradient end of the flow path.

#### 4.2. Mass-transfer modeling

Mass transfer of carbon, oxygen, iron and sulfur

Table 5

Chemical equations used to describe reactions in the Magothy aquifer, Suffolk County, NY

*Organic carbon oxidation**Mass transfer*

$$\Delta M_C = m_{\text{CO}_2} \quad (5)$$

$$R_p = \Delta M_C v / L, \text{ where :} \quad (6)$$

$$R_p = \text{rate of CO}_2 \text{ production, in mmol l}^{-1} \text{ yr}^{-1} \quad (6a)$$

$$v = \text{velocity of groundwater flow, in m yr}^{-1} \quad (6b)$$

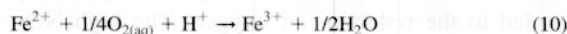
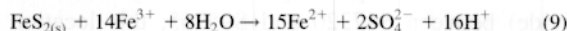
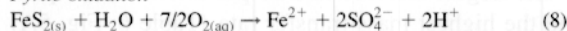
$$L = \text{flow path length, in m} \quad (6c)$$

$$\Delta S = (S_{\text{FeS}_2\text{ox}} + S_{\text{diff}}) - S_{\text{SO}_4\text{red}} = \Delta S_{\text{SO}_4^{2-}}, \text{ where :} \quad (7)$$

$$S_{\text{FeS}_2\text{ox}} = \text{mass of sulfur from FeS}_2 \text{ oxidation} \quad (7a)$$

$$S_{\text{diff}} = \text{mass of sulfur leached by diffusion from poorly permeable sediments} \quad (7b)$$

$$S_{\text{SO}_4^{2-}\text{red}} = \text{SO}_4^{2-} \text{ removed by reduction of SO}_4^{2-}, \text{ which can react with iron to form FeS}_2 \quad (7c)$$

*Pyrite oxidation**Sulfur mass transfer*

$$\Delta \delta^{34}\text{S} = (m_{\text{FeS}_2\text{ox}} \delta^{34}\text{S}_{\text{FeS}_2\text{ox}} + m_{\text{Sdiff}} \delta^{34}\text{S}_{\text{diff}}) - m_{\text{S}_{\text{atm}}} \delta^{34}\text{S}_{\text{atm}} = \Delta m_{\text{SO}_4} \delta^{34}\text{S}_{\text{SO}_4} \quad (11)$$

Table 5 (continued)

$$\Delta \text{SO}_4^{2-} = (\text{SO}_4^{2-} \text{ FeS}_{2\text{ox}} + \text{SO}_4^{2-} \text{ diff}) - \text{SO}_4^{2-} \text{ red} \quad (12)$$

*Sulfate reduction*

$$\text{SO}_4^{2-} \text{ red} = (\text{SO}_4^{2-} \text{ FeS}_{2\text{ox}} + \text{SO}_4^{2-} \text{ diff}) - \text{SO}_4^{2-} \text{ mass transfer} \quad (13)$$

*CO<sub>2</sub> production*

$$\text{CO}_{2\text{SO}_4} = 2 \cdot \text{SO}_4^{2-} \text{ red} \quad (14)$$

$$\text{CO}_{2\text{O}_2} = \text{O}_2 \quad (15)$$

$$\text{CO}_{2\text{FeIII}} = 4 \cdot \text{Fe(II)} \quad (16)$$

along the modeled flow path from the groundwater divide south to the barrier island (Fig. 1) was studied to identify spatial trends and local chemical processes. Data from several of the wells were selected for computation of mass transfer rates (Figs. 1 and 2). Major element and chemical-species concentrations and stable isotope compositions of sulfur and carbon species in water samples from 17 wells are given in Table 4. Mass-transfer rates for carbon, oxygen, iron and sulfur between several points along the flow path were calculated from estimated rates of mass transfer and groundwater flow. Mass-transfer rates could not always be determined for each constituent along the same flow path segments because of interferences from anthropogenic effects or steel well screens. In such cases, a nearby well was substituted for the problem well. Major constituents that were not involved in redox reactions, including  $\text{Na}^+$ ,  $\text{Ca}^{2+}$ ,  $\text{Mg}^{2+}$  and  $\text{Cl}^-$ , showed minor concentration changes associated with clay-mineral weathering and ion exchange along the flow path (Brown, 1998).

*4.2.1. Carbon*

The increase in dissolved inorganic carbon (DIC) along the flow path (Fig. 3D) is consistent with oxidation of SOM coupled to the reduction of oxygen, Fe(III) and  $\text{SO}_4^{2-}$ . The values for  $\delta^{13}\text{C}$  of DIC, which are isotopically light in the recharge area, remain light along the flow path (Fig. 6) despite the doubling of DIC values and support the oxidation of the isotopically light lignite as the source for the DIC

increase. Dissolved oxygen in the aerobic part of the Magothy is a major electron acceptor for production of DIC and can be represented by Eq. (1) (Table 5). One mole of  $O_2$ , therefore, is consumed for every mole of  $CO_2$  that is produced. Calcite dissolution is unlikely to contribute to the DIC increase because the Magothy contains little or no carbonate minerals (Pearson and Friedman, 1970).

The trend of DIC along the modeled flow path (Fig. 3D) indicates an increase of DIC in both the aerobic zone and in the anaerobic zone. Locally high concentrations of DIC in aerobic parts of the Magothy probably result from human activities, such as liming and sewerage. Water from wells S34031, S47886 and S47887 had relatively high concentrations of DIC that may result from locally rapid oxidation of lignite; the associated low pH probably results from oxidation of  $FeS_2$  caused by drawdown of shallow, oxygenated waters. Oxygen reduction is probably the major TEAP that is coupled to the oxidation of lignite in the aerobic zone. Sulfate reduction occurs in anaerobic microenvironments within the aerobic part of the Magothy aquifer (Brown et al., 1999), however, and contributes to the oxidation of SOM and to the overall DIC increase along the modeled flow path. Anaerobic microenvironments in aerobic parts of the Middendorf aquifer of South Carolina were described by Murphy et al. (1992), and zones with the highest SOM had relatively low populations of aerobic heterotrophs (Fredrickson et al., 1991).

The rate of DIC increase beyond about 8–10 km along the flow path, where groundwater becomes anaerobic, probably reflects Fe(III) reduction and  $SO_4^{2-}$  reduction as the dominant TEAPs that are coupled to lignite oxidation. Oxidation of organic matter by iron reduction can be represented by Eqs. (2) and (3) (Table 5). The low solubility of Fe(III) may require Fe(III)-reducing organisms to come into direct contact with Fe(III)-bearing solids (Lovley, 1987) unless either the Fe(III) is complexed with other compounds (e.g. Lovley et al., 1996), or the pH is low enough ( $< \sim 3$ ) that Fe(III) is soluble. Only 1 mol of bicarbonate is produced for every 4 mol of  $Fe(OH)_3(s)$  that are reduced; therefore, a large amount of ferrous iron can be produced by oxidation of a small amount of lignite. The oxidation of organic matter by  $SO_4^{2-}$  reduction, represented by

Eq. (4) (Table 5), produces 2 mol of bicarbonate for every mole of  $SO_4^{2-}$  that is reduced.

The mass of  $CO_2$  produced through oxidation of organic matter within four segments of the modeled flow path was estimated to range from 0.071 to 0.402  $mmol\ l^{-1}$  as C, with a total of 0.763  $mmol\ l^{-1}$  for the entire length of the flow path (Fig. 1 and Table 6). The change in DIC concentration along a flow path segment can be represented by Eq. (5) (Table 5), where  $m_{CO_2}$  is the concentration of  $CO_2$ . The annual rate of  $CO_2$  production from lignite oxidation in the Magothy aquifer was calculated from Eq. (6).

Mass transfer in the recharge area between two wells within a cluster at the groundwater divide (S47220 and S95965) was calculated with vertical groundwater velocities of 1.1–11.1  $m\ yr^{-1}$  (Buxton and Modica, 1992). Carbon dioxide production rates between wells farther along the flow path were estimated from published horizontal hydraulic conductivity values (Table 6) for the Magothy aquifer in Suffolk County, which range from  $5.35 \times 10^{-3}$  to  $6.10 \times 10^{-3}\ m\ yr^{-1}$  (McClymonds and Franke, 1972). The estimated rates of  $CO_2$  production from organic matter (lignite) oxidation (Table 6; Fig. 5A) ranged from  $2.55 \times 10^{-4}$  to  $4.86 \times 10^{-3}\ mmol\ l^{-1}\ yr^{-1}$  and are comparable to those obtained from geochemical modeling in the Magothy/Upper Patapsco aquifer of Maryland ( $10^{-4}$  to  $10^{-3}\ mmol\ l^{-1}\ yr^{-1}$ ; Chappelle et al., 1987), and the upper range of values obtained for the Lower Patapsco aquifer of Maryland ( $10^{-5}$  to  $10^{-4}\ mmol\ l^{-1}\ yr^{-1}$ ; Chappelle et al., 1987), and the Madison aquifer system in parts of Wyoming, Montana, and South Dakota ( $10^{-6}$  to  $10^{-3}\ mmol\ l^{-1}\ yr^{-1}$ ; Plummer, 1988), but are considerably higher than the simulated rates for the Black Creek, Middendorf and Cape Fear aquifers of South Carolina ( $10^{-6}$  to  $10^{-5}\ mmol\ l^{-1}\ yr^{-1}$ ; Chappelle and Lovley, 1990).

The largest increase in DIC per meter of flow path and the highest mass-transfer rate (Table 6; Fig. 5A) was in the first flow-path segment (at the groundwater divide) between S47220 and S95965; this location indicates that the oxidation of lignite is primarily coupled to the reduction of oxygen. The high  $NO_3^-$  concentration ( $0.037\ mmol\ l^{-1}$  as N) in water from the latter well is probably derived from human activities — Buxton and Modica (1992) found a strong correlation between nitrate concentrations (which can be related to effects of human activity since the

Table 6

Hydraulic values used in calculation of mass-transfer rates of CO<sub>2</sub>, O<sub>2</sub>, Fe(II), and SO<sub>4</sub><sup>2-</sup> in segments of Magothy aquifer flow path ( $\Delta M_x$ , mass-transfer rate of constituent x, numbers in parentheses are based on flow rates given in Buxton and Modica (1992). Aquifer porosity ( $n_a$ ) = 0.25 (Faust, 1963). Dashes indicate value was not calculated)

Flow-path segment (a)	Computation of $\Delta M_x$ per meter (b/c)			Computation of groundwater velocity ( $e \times f/0.25$ )			Mass-transfer rate (mmol l <sup>-1</sup> yr <sup>-1</sup> $\times 10^{-4}$ ) (d $\times$ g)
	$\Delta$ concentration (mmol l <sup>-1</sup> ) (b)	Flow-path length (m) (c)	$\Delta M_x$ per meter of flow path $\times 10^{-6}$ (d)	Hydraulic conductivity (m yr <sup>-1</sup> ) (e)	Hydraulic gradient ( $\times 10^{-3}$ ) (f)	Groundwater velocity (m yr <sup>-1</sup> ) (g)	
<i>CO<sub>2</sub> production</i>							
(1) S47220-S95965	0.071	160	438	-	-	1.11-11.1 <sup>ab</sup>	4.86-48.6 (9.11)
(2) S95965-S75034	0.242	6,460	37.4	5,350-6,100	0.768	16.4-18.7	6.16-7.02
(3) S75034-S22351	0.048	6,940	6.92	5,350-6,100	1.72	36.8-42.0	2.55-2.90
(4) S22351-S36803	0.402	6,960	57.8	5,350-6,100	0.289	6.18-7.05	3.57-4.07
(T) S47220-S36803	0.763	20,520	37.2	5,350-6,100	1.5	32.1-36.6	11.9-13.6
<i>O<sub>2</sub> consumption</i>							
(1) S95963-S95965	0.184	130	1,424	-	-	1.11-11.1 <sup>ab</sup>	15.8-158 (29.6)
(2b) S95964-S75034	0.132	6,500	20.2	5,350-6,100	1.05	22.5-25.6	4.54-5.17
(2a) S95965-S75034	0.0156	6,460	2.42		0.78	16.7-18.7	0.404-0.453
(3) S75034-S47887	0.084	6,750	12.45	5,350-6,100	1.65	35.2-40.2	4.38-5.00
(4) S47887-S36803	0.0018	7,150	0.262	5,350-6,100	0.406	8.68-9.91	0.0228-0.0260
(T) S95963-S47887	0.284	13,340	21.3	5,350-6,100	1.39	29.8-33.9	6.33-7.22
<i>Fe(II) production</i>							
(1) S95963-S95964	-0.00005	70	-0.816	-	-	1.11-11.1 <sup>ab</sup>	-0.0091 to -0.091 (-0.017)
(2) S95964-S74586	0	6,440	0	5,350-6,100	1.37	22.2-25.3	0
(3) S74586-S22351	0.0108	7,020	1.54	5,350-6,100	1.75	37.5-42.7	0.575-0.656
(4) S22351-S36803	0.00895	6,960	1.29	5,350-6,100	0.289	6.18-7.05	0.079-0.091
(T) S95963-S36803	0.0197	20,480	0.961	5,350-6,100	1.03	22.0-25.1	0.212-0.242
<i>SO<sub>4</sub><sup>2-</sup> production</i>							
(1) S95963-S95965	0.0097	130	74.7	-	-	1.11-11.1 <sup>ab</sup>	0.829-8.29 (1.55)
(2) S95965-S75034	-0.0031	6,460	-0.483	5,350-6,100	0.768	16.4-18.7	-0.079-0.091
(3) S75034-S47887	0.0167	6,750	2.47	5,350-6,100	1.65	35.2-40.2	0.869-0.991
(4) S47887-S36803	0.0375	7,150	5.24	5,350-6,100	0.406	8.68-9.91	0.455-0.519
(T) S95963-S36803	0.0607	20,480	2.96	5,350-6,100	1.03	22.0-25.1	0.653-0.744

<sup>a</sup> From Buxton and Modica (1992).

<sup>b</sup> Value is 2.08 m yr<sup>-1</sup> when based on assumptions from Buxton and Modica (1992), as described in text.

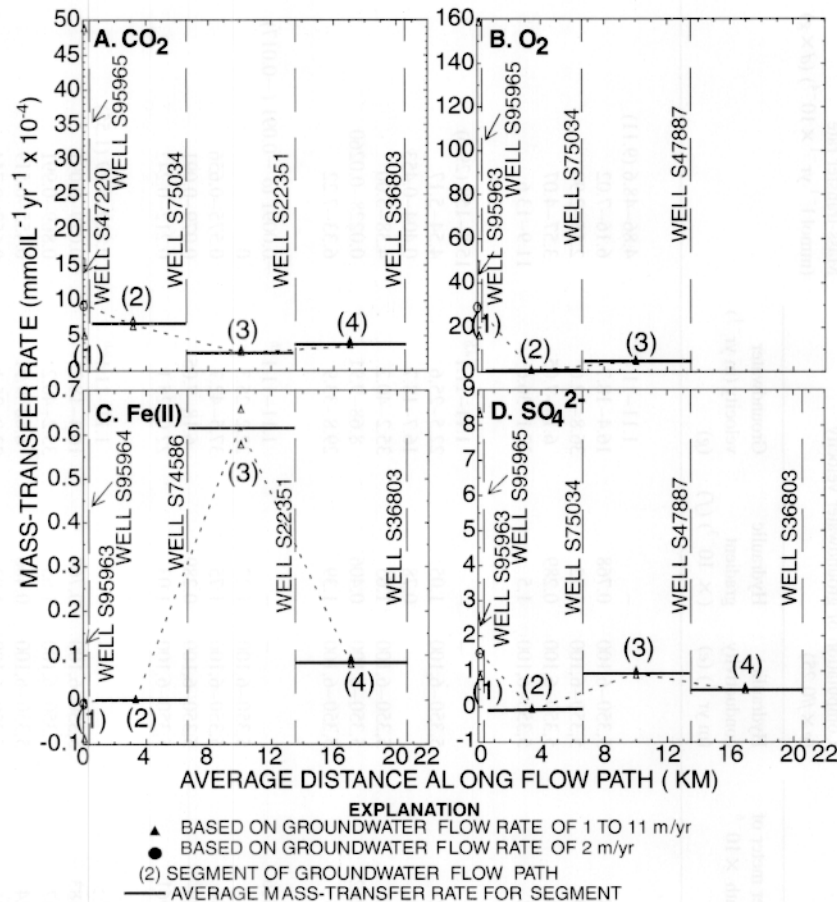


Fig. 5. Estimated mass-transfer rates of dissolved (A)  $\text{CO}_2$ , (B)  $\text{O}_2$ , (C)  $\text{Fe(II)}$ , and (D)  $\text{SO}_4^{2-}$  along segments of Magothy flow path.

early 1900s), and the 75-yr age line defined by their flownet and traveltime analyses, and concluded that every well screened in water older than 75 yr had nitrate concentrations less than or equal to  $0.037 \text{ mmol l}^{-1}$  as N. Therefore, if nitrate reduction is assumed to occur at a relatively constant rate, water at the screen zone of well S95965 is no less than 75 yr old, and flow rates in this zone would be no greater than  $2.08 \text{ m yr}^{-1}$ . This revised flow-rate estimate narrows the range of mass-transfer rates in the first flow-path segment (Table 6; Fig. 5A).

The second highest mass-transfer rate was along the second flow-path segment (S95965 to S75034), which also is predominantly aerobic (Table 6). The high mass-transfer rate of  $\text{CO}_2$  relative to the  $\text{O}_2$  consumption rates suggests that production rates of  $\text{SO}_4^{2-}$  and

$\text{Fe(II)}$  were actually higher than is indicated by groundwater chemistry. The oxidation of lignite and the resulting production of  $\text{CO}_2$  with distance from the groundwater divide should correspond with the consumption of electron acceptors, including  $\text{O}_2$ ,  $\text{Fe(III)}$  and  $\text{SO}_4^{2-}$ . Concentrations of  $\text{Fe(II)}$  increase, as expected from  $\text{Fe(III)}$  reduction, but the decrease in  $\text{SO}_4^{2-}$  concentrations typically expected with  $\text{SO}_4^{2-}$  reduction is masked (Fig. 3C) by the increase in  $\text{SO}_4^{2-}$  leaching from silt and clay (Brown et al., 1999).

The  $\delta^{13}\text{C}$  values for DIC in groundwater samples range from  $-22.2$  to  $-21.0\text{‰}$ ; these are somewhat "heavier" than  $\delta^{13}\text{C}$  values for lignite samples from Magothy sediments ( $-24.3$  to  $-22.5\text{‰}$ ; Table 7) and the value for groundwater at a recharge area ( $-25\text{‰}$ ) reported by Pearson and Friedman (1970), perhaps

Table 7

$\delta^{34}\text{S}$  of  $\text{FeS}_2$  samples and  $\delta^{13}\text{C}$  of lignite samples from core samples at the four borehole sites (borehole locations shown in Fig. 1, altitudes in meters from sea level)

ID	Borehole location <sup>a</sup>	Sample altitude	$\delta^{34}\text{S}$	Sample description
<i>Iron-sulfide mineral samples</i>				
IS-1	AD	-109.6	-36.3	Marcasite-cemented sand
IS-2	LA	-146.9	-28.2	Pyrite-replaced lignite
IS-3	LO	-118.0	8.41	Marcasite-cemented sand
IS-4	LO	-158.8	10.6	Pyrite-replaced lignite
IS-5	LO	-159.4	-3.52	Marcasite-cemented sand
IS-6	MA	-141.5	-40.2	Marcasite-cemented sand
IS-7	MA	-142.1	-44.1	Pyrite-replaced lignite
IS-8	MA	-166.8	-25.0	Pyrite-replaced lignite
IS-9	MO	-197.1	-1.94	Marcasite- and pyrite-cemented sand
<i>Lignite samples</i>			$\delta^{13}\text{C}$	
LI-1	AD	-109.6	-23.49	Lignite
LI-2	AD	-117.2	-22.93	Lignite
LI-3	LA	-146.9	-24.26	Lignite
LI-4	LO	-118.0	-22.54	Lignite
LI-5	MA	-142.4	-23.83	Lignite
LI-6	MA	-175.6	-23.99	Lignite

<sup>a</sup> AD, Adams Ave. LA, Landscape Dr. LO, Locust Dr. MA, Margin Dr.

this is because the samples contained a greater contribution from atmospheric  $\text{CO}_2$  ( $-7\text{‰}$ ) or because human-related activities, such as soil liming, contribute DIC from calcite or dolomite ( $0\text{‰}$ ). The  $\delta^{13}\text{C}$  range of DIC was only  $1.2\text{‰}$ , and despite minor variations along the flow path (Fig. 6), the local differences were not much more than the precision of the analysis ( $0.2\text{‰}$ ). The  $\delta^{13}\text{C}$  of DIC initially decreases with depth in the recharge area and reaches  $-21.6\text{‰}$  well S95964. Well S34031, which is located to the east and about 4 km south of the divide (Figs. 1 and 2), has the

lowest  $\delta^{13}\text{C}$  value of  $-22.2\text{‰}$  (Fig. 6); this lighter  $\delta^{13}\text{C}$  of DIC could be caused by autotrophs such as *Thiobacillus ferrooxidans*, a pyrite oxidizer (Cravotta, 1998) that can fix  $\text{CO}_2$  in the aerobic zone and cause depletion of  $^{13}\text{C}$  in DIC. Aerobic heterotrophs also can deplete  $^{13}\text{C}$  in DIC by oxidation of organic carbon; Blair et al. (1985) measured a  $3.4\text{‰}$  depletion in the  $\delta^{13}\text{C}$  of  $\text{CO}_2$  respired by *E. Coli* relative to  $\text{CO}_2$  in its glucose substrate. Farther along the flow path,  $\delta^{13}\text{C}$  of DIC becomes enriched and remains at about  $-21.2\text{‰}$ , a value similar to those for the Middendorf aquifer of

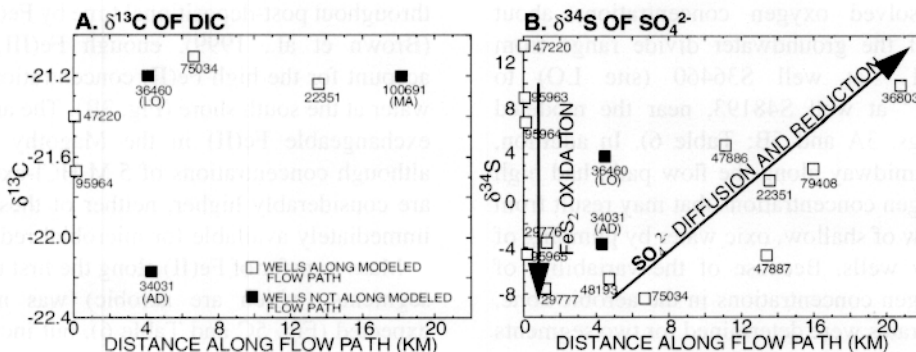


Fig. 6. Isotope composition of groundwater along Magothy flow path from the groundwater divide: A.  $\delta^{13}\text{C}$  of DIC. B.  $\delta^{34}\text{S}$  of  $\text{SO}_4^{2-}$ .

South Carolina (Murphy et al., 1992). Even though carbon isotopes, theoretically, should not fractionate during reduction of Fe(III) or  $\text{SO}_4^{2-}$  by acetate because both carbon molecules in the acetate generally are converted to  $\text{CO}_2$  (Murphy et al., 1992), the low  $\delta^{13}\text{C}$  values in basal Magothy groundwater probably results from some form of fractionation associated with lignite oxidation, because  $\delta^{13}\text{C}$  of lignite is relatively "light" compared to that of DIC in groundwater and because carbon from calcite is absent in the Magothy aquifer. The  $\text{CO}_2$  in water from deep coastal-plain aquifers in South Carolina was enriched in  $^{13}\text{C}$  by about 5‰ relative to  $\text{CO}_2$  in water from updip sediments and only part of this enrichment could be attributed to local variability in isotopic composition of the SOM (McMahon et al., 1990). Fractionation may result from differences between the degradability of aliphatic and aromatic compounds of SOM under aerobic conditions and that under anaerobic conditions.

#### 4.2.2. Oxygen

Dissolved oxygen concentrations decrease from 0.288  $\text{mmol l}^{-1}$  at the recharge area (S95963) to below 0.003  $\text{mmol l}^{-1}$  about 11 km downgradient at S47886 (Fig. 3A). The position of the dissolved oxygen front in the Magothy aquifer is affected by the distribution and abundance of SOM in the Magothy and by the permeability of sediments along individual flow paths, although gradients induced by water-supply pumping during the past 50 yr has caused localized mixing of deep groundwater with shallow, oxygenated water in some areas (Bennett et al., 1996). As a result,  $\text{O}_2$  concentrations and mass-transfer rates vary locally along the flow path. For example, dissolved oxygen concentrations about 5 km south of the groundwater divide range from 0.0016  $\text{mmol l}^{-1}$  at well S36460 (site LO) to 0.125  $\text{mmol l}^{-1}$  at well S48193, near the modeled flow path (Figs. 3A and 5B; Table 6). In addition, well S75034, midway along the flow path, had high dissolved oxygen concentrations that may result from downward flow of shallow, oxic water by pumping of nearby supply wells. Because of the variability of dissolved oxygen concentrations in the aerobic zone, mass-balance rates were determined for two segments of flow path 2: S95964 to S75034 (flow-path 2a) and S95965 to S75034 (flow-path 2b; Table 6). The mass-

transfer (or "consumption") rates of dissolved oxygen in the Magothy were estimated in the same manner as  $\text{CO}_2$  production rates (Eq. (6), Table 5) and ranged from 4.86 to  $48.6 \times 10^{-4} \text{ mmol l}^{-1} \text{ yr}^{-1}$  near the divide (S95963 to S95965), and ranged from  $6.33 \times 10^{-4}$  to  $7.22 \times 10^{-4} \text{ mmol l}^{-1} \text{ yr}^{-1}$  along the entire aerobic segment of the flow path (S95963 to S47887). These latter rates are lower than those calculated for the organic-rich Hawthorne aquifer in South Carolina ( $10^{-2} \text{ mmol l}^{-1} \text{ yr}^{-1}$ ; Chapelle, 1993) but are close to the values calculated for the Patuxent aquifer in the coastal plain of Maryland (about  $10^{-4} \text{ mmol l}^{-1} \text{ yr}^{-1}$ ; Chapelle, 1993).

#### 4.2.3. Iron

The net rate of Fe(II) mass transfer along the modeled flow path from S95963 at the divide to S36803 on the barrier island was estimated to range between  $0.212 \times 10^{-4}$  and  $0.242 \times 10^{-4} \text{ mmol l}^{-1} \text{ yr}^{-1}$ , although much of the Fe(II) is sequestered in sediments and probably results in significant underestimation of Fe(II) mass transfer. Most of the dissolved iron is produced under anaerobic conditions by Fe(III)-reducing organisms, which couple the oxidation of organic matter to Fe(III) reduction (Lovley et al., 1990) and release Fe(II) and bicarbonate to solution (Eqs. (2) and (3), Table 5). Amorphous or poorly ordered Fe(III) oxyhydroxide is considered microbially reducible (Chukhrov et al., 1973; Lovley and Phillips, 1986a), whereas other iron forms, including  $\text{Fe}_2\text{O}_3$  (hematite) and  $\text{Fe}_3\text{O}_4$  (magnetite), are not (Lovley and Phillips, 1986b). The amount of Fe(III) oxyhydroxide coating on Magothy sediments is small ( $<0.1\text{--}0.28 \mu\text{g g}^{-1}$ ), and even though they probably have been depleted throughout post-depositional time by Fe(III) reduction (Brown et al., 1999), enough Fe(III) remains to account for the high Fe(II) concentrations in groundwater at the south shore (Fig. 3B). The amount of ion-exchangeable Fe(II) in the Magothy also is low; although concentrations of 5 M HCl-extractable iron are considerably higher, neither of these fractions is immediately available for microbial reduction.

Mass transfer of Fe(II) along the first two flow-path segments (which are aerobic) was negligible, as expected (Fig. 5C and Table 6), but increased downgradient. A significant amount of iron in  $\text{FeS}_2$  minerals is released in aerobic parts of the aquifer by

oxidative dissolution, as discussed later, but generally is tied up in sediments. Well S74586, midway along the flow path (Figs. 1 and 2) was selected as a study point for Fe(II) mass-balance modeling in place of well S75034 (at the same location), which was contaminated by iron from the steel casing. The third flow-path segment (S74586 to S22351) had the largest Fe(II)-production rate, but this does not account for the high CO<sub>2</sub>-production rate (Table 6) because 4 mol of Fe(III) are required to oxidize 1 mol of CO<sub>2</sub> (Eq. (2), Table 5), and this amount ( $0.144 \times 10^{-4}$  to  $0.164 \times 10^{-4}$  mmol l<sup>-1</sup> yr<sup>-1</sup>) would account for only 5–6% of the CO<sub>2</sub> produced. Thus, because O<sub>2</sub> reduction is negligible in the anaerobic parts of the flow path, SO<sub>4</sub><sup>2-</sup> reduction and Fe(III) reduction that is not reflected in Fe(II) mass transfer values may account for the remainder of the CO<sub>2</sub> production through lignite oxidation. The last flow-path segment (S22351 to S36803) had a relatively lower mass-transfer rate than the third segment (Fig. 5C; Table 6) as a result of its lower hydraulic gradient and slower flow rates than in the third segment.

#### 4.2.4. Sulfur

Sulfur in the Magothy aquifer is derived from SO<sub>4</sub><sup>2-</sup> in atmospheric deposition, from oxidation of FeS<sub>2</sub> minerals, and from SO<sub>4</sub><sup>2-</sup> diffusion from poorly permeable sediments within the Magothy aquifer. The increase in total sulfur ( $\Delta S$ ) along the flow path from the point of recharge can be represented by Eq. (7) (Table 5). Sulfate is the major form of sulfur in water from wells; therefore,  $\Delta S = \Delta SO_4^{2-}$ . Low aqueous-sulfide concentrations (<0.25–0.7 μmol l<sup>-1</sup> as H<sub>2</sub>S) in water from wells in the anaerobic part of the flow path indicate that Fe(II) in the water reacts with sulfide to form FeS<sub>2</sub>.

An overall increase in SO<sub>4</sub><sup>2-</sup> concentrations downward along the flow path from S95963, near the divide, to S36803 at the southern barrier island indicates that much more SO<sub>4</sub><sup>2-</sup> is produced by leaching of SO<sub>4</sub><sup>2-</sup> in poorly permeable zones and through pyrite oxidation than is removed by SO<sub>4</sub><sup>2-</sup> reduction and mineral precipitation. Sulfate concentrations showed an overall increase along the first flow-path segment (S95963 to S95965) and SO<sub>4</sub><sup>2-</sup>-production rates were from 0.829 to  $8.29 \times 10^{-4}$  mmol l<sup>-1</sup> yr<sup>-1</sup>, but showed little or no further increase until the end of the second

segment (S75034), where anaerobic conditions predominate (Figs. 3C and 6D; Table 6). Sulfate concentrations again increased along the third and fourth flow-path segments and the relatively high mass transfer values may result from the southward lithologic progression from a predominantly transitional-nonmarine depositional environment of Magothy sediments at the center of the Long Island, to some area of increasing marine influence near the south shore with a transitional-marine depositional environment. Clay lenses could have retained the anion-exchange complex from this marine influence either during sediment deposition or during sea transgression at a later time (Brown, 1998). The fourth flow-path segment had a higher mass transfer than the third segment, but a lower SO<sub>4</sub><sup>2-</sup>-production rate because it has a lower hydraulic gradient and, therefore, slower flow rates (Table 6).

The δ<sup>34</sup>S of SO<sub>4</sub><sup>2-</sup> in the Magothy was used to determine the sources and processes associated with sulfur, including the increase of sulfate concentrations in the anaerobic zone. The trend of δ<sup>34</sup>S of SO<sub>4</sub><sup>2-</sup> along the modeled flow path consists of an abrupt decrease near the divide, followed by a more gradual increase with distance toward the south shore (Fig. 6B). The δ<sup>34</sup>S of SO<sub>4</sub><sup>2-</sup> is “heavy” (about 13‰) at the shallowest well (S47220) in the recharge area and is indicative of atmospheric SO<sub>4</sub><sup>2-</sup>-the δ<sup>34</sup>S of atmospheric precipitation ranges from about 20‰ in regions containing only sea-spray SO<sub>4</sub><sup>2-</sup> to about 0‰ in highly industrialized regions (Coplen, 1993); therefore, recharge at S47220 probably represents a mixture of SO<sub>4</sub><sup>2-</sup> from both sources. Groundwater moving downgradient from the point of recharge abruptly becomes “lighter” with depth (about -8‰ at S75034), probably as a result of the oxidative dissolution of FeS<sub>2</sub> (pyrite or marcasite). Oxidative dissolution of isotopically “light” pyrite and/or marcasite in sediments near the recharge area (such as IS-1 and IS-2, Table 7) could cause the shift to depleted δ<sup>34</sup>S of SO<sub>4</sub><sup>2-</sup> within 4 km of the recharge area (Fig. 6B). Because initial SO<sub>4</sub><sup>2-</sup> concentrations are low, and because sulfide oxidation does not produce significant fractionation (Taylor et al., 1984), only a small addition of “light” sulfur is needed to cause the depletion. In contrast, SO<sub>4</sub><sup>2-</sup> reduction can produce significant fractionation of 30–60‰ (Canfield et al., 1992) because SO<sub>4</sub><sup>2-</sup>-reducing organisms along a flow path

will preferentially metabolize the lighter isotope ( $^{32}\text{S}$ ). Therefore,  $\text{FeS}_2$  minerals typically are depleted in  $\delta^{34}\text{S}$  and the remaining dissolved  $\text{SO}_4^{2-}$  becomes enriched in  $^{34}\text{S}$ . The effect of this enrichment through isotopic fractionation is enhanced in poorly permeable sediments that can act as a closed system in which mixing with other water is minimal. In addition,  $^{34}\text{S}$ -enriched  $\text{SO}_4^{2-}$  from connate sea water is probably desorbed from clayey sediments (Brown, 1998). Consequently, the  $\delta^{34}\text{S}$  compositions of pyrite and marcasite from Magothy aquifer boreholes vary widely (from  $-44.1$  to  $10.6\%$ ; Table 7). Water from S47887 has a lower  $\delta^{34}\text{S}$  ( $-4.7\%$ ) than other waters at similar distances along the flow path (Fig. 6B); this, together with the low pH (4.44) of these waters, indicate the oxidation of  $\text{FeS}_2$ .

Pyrite oxidation can be represented by either of the reactions described in Eqs. (8) or (9).  $\text{Fe(III)}$  has been found to be the more effective oxidant of pyrite (Eq. (9), Table 5) in laboratory experiments, but oxidation of  $\text{Fe(II)}$  to  $\text{Fe(III)}$  requires dissolved oxygen (Eq. (10)) (McKibben and Barnes, 1986; Moses et al., 1987). Substituting  $\delta^{34}\text{S}$  for S in Eq. (7) and subtracting the sulfate derived from precipitation recharge ( $m_{\text{Satm}}\delta^{34}\text{S}_{\text{atm}}$ ) yields Eq. (11).

The  $\delta^{34}\text{S}$  value of pyrite is generally "light" in the upper sediments near the recharge area, as represented by pyrite from Landscape Dr. (IS2) and by marcasite from Adams Ave. (IS1) (Table 7). Results of geochemical mass-balance modeling with NETPATH for estimates of  $\text{FeS}_2$  oxidation from  $\delta^{34}\text{S}$  values (Brown, 1998) were revised to reflect several multiple flow-path segments in the aerobic zone and yielded a range from 40 to 84% of the  $\text{SO}_4^{2-}$  that is derived from the oxidation of  $\text{FeS}_2$ . The increase in  $\delta^{34}\text{S}$  of  $\text{SO}_4^{2-}$  after its initial decrease (Fig. 6B) probably results from: (1) infusion of "heavier" seawater-derived  $\text{SO}_4^{2-}$  desorbed from poorly-permeable sediments; and (2)  $\text{SO}_4^{2-}$  reduction and the subsequent formation of  $\text{FeS}_2$ . Assuming that a source of heavy sulfate is derived from sea water, some oxidation of  $\text{FeS}_2$  is necessary to give the  $^{34}\text{S}$  of  $\text{SO}_4^{2-}$  value of  $9.8\%$  found at S36803. Results of geochemical mass-balance modeling for estimates of  $\text{FeS}_2$  oxidation along an anaerobic part of the modeled flow path (Brown, 1998) were revised using several flow-path segments and yielded a range from 19 to 34%. Pyrite can be oxidized by dissolved ferric ions under low pH

conditions (Eq. (9), Table 5), provided that oxygen is present initially to begin the reaction (Eq. (8)) and to produce acid.

The nonuniform distribution of pore-water  $\text{SO}_4^{2-}$ , sediment texture, and SOM is evident through a chemical comparison ( $\delta^{34}\text{S}$  of  $\text{SO}_4^{2-}$  and iron concentrations) in water from two wells at similar distances from the groundwater divide. Water from supply well S48193, 4.6 km south of the groundwater divide (Fig. 1), has a "light"  $\delta^{34}\text{S}$  of  $-6.7\%$ , water from supply well S36460 at site LO, 4.1 km south of the divide (Fig. 1) along a parallel flow path about 13 km east of the modeled one, has a relatively "heavy"  $\delta^{34}\text{S}$  of  $3.9\%$ . Although the two flow paths cannot be compared directly, the much heavier  $\delta^{34}\text{S}$  at S36460 than at S48193 would be consistent with the greater  $\text{SO}_4^{2-}$ -reducing activity at site LO despite the somewhat shorter flow path. The  $\delta^{34}\text{S}$  compositions of pyrite and marcasite samples from site LO are also much "heavier" than those of corresponding samples from sites LA and MA (Table 7), or of samples formed in open systems. Clay lenses are present at several depths in Magothy sand at site LO and can form isolated microenvironments in the sand in which  $^{32}\text{S}$  of pore water becomes depleted with increasing depth and (or) time, and the residual  $\text{SO}_4^{2-}$  becomes progressively enriched in  $^{34}\text{S}$ . Reduction of this "heavy"  $\text{SO}_4^{2-}$ , and its subsequent reaction with  $\text{Fe(II)}$ , would form  $\text{FeS}_2$  minerals that are enriched in  $^{34}\text{S}$ .

The unknown  $\text{SO}_4^{2-}$  flux from clays makes the relative contribution of  $\text{SO}_4^{2-}$  as an electron acceptor for the oxidation of lignite difficult to determine. The  $\text{SO}_4^{2-}$  mass transfer can be described in Eq. (12) by rearranging Eq. (7) (Table 5). Sulfate reduction can be estimated by first calculating the rate of  $\text{SO}_4^{2-}$  diffusion. Chappelle and McMahon (1991) accounted for a deficit of electron acceptors in the Black Creek aquifer of South Carolina by estimating rates of  $\text{SO}_4^{2-}$  leaching from marine beds on the assumption that this  $\text{SO}_4^{2-}$  is sufficient to account for observable  $\text{CO}_2$  production in the system. These estimates also assume that the rate of  $\text{SO}_4^{2-}$  diffusion greatly exceeds the rate of  $\text{SO}_4^{2-}$  removal through advection and that  $\text{SO}_4^{2-}$  diffusing from sediments is continuously utilized by  $\text{SO}_4^{2-}$ -reducing bacteria. The  $\text{SO}_4^{2-}$ -diffusion flux was estimated in the present study through Fick's first law and using  $\text{SO}_4^{2-}$ -concentration gradients from

Table 8

Rates of  $\text{SO}_4^{2-}$  reduction and  $\text{CO}_2$  production, as estimated from  $\text{SO}_4^{2-}$  diffusion,  $\text{SO}_4^{2-}$ -mass transfer, and  $\text{FeS}_2$  oxidation at three sampling sites in the Magothy aquifer (borehole locations shown in Fig. 1)

Sample location	Rates ( $\text{mmol l}^{-1} \text{yr}^{-1} \times 10^{-4}$ )				
	$\text{SO}_4^{2-}$ diffusion <sup>a</sup>	$\text{SO}_4^{2-}$ mass transfer	$\text{FeS}_2$ oxidation <sup>b</sup>	$\text{SO}_4^{2-}$ reduction	$\text{CO}_{2(\text{SO}_4)}$ production
<i>Near recharge area, aerobic</i>					
LA3/LA2	0.320–3.9	0.233–0.266	0.158–0.181	0.148–3.89	0.296–7.78
LA3/LA1					
<i>Near south shore, anaerobic</i>					
LO1/LO2	1.07–6.15	0.455–0.519	0.086–0.176	0.064–5.87	1.27–11.7
MA4/MA2					

<sup>a</sup> Details of  $\text{SO}_4^{2-}$ -diffusion calculations presented in Brown (1998).

<sup>b</sup> Estimated to be 40–84% in the aerobic zone and 19–34% in the anaerobic zone (revised from Brown, 1998).

pore-water chemistry data (Table 3), as described in Brown (1998). Resulting values ranged from  $0.320 \times 10^{-4}$  to  $3.90 \times 10^{-4} \text{ mmol l}^{-1} \text{yr}^{-1}$  near the recharge area (site LA) and from  $1.07 \times 10^{-4}$  to  $6.15 \times 10^{-4} \text{ mmol l}^{-1} \text{yr}^{-1}$  near the south shore (site MA) (Table 8). The  $\text{SO}_4^{2-}$ -diffusion flux was then equated to  $\text{CO}_2$  production rates (Table 8).

#### 4.2.5. Oxidation of SOM

The amount of reduction of dissolved oxygen,  $\text{SO}_4^{2-}$  and  $\text{Fe(III)}$  that is required for production of the observed  $\text{CO}_2$  along the modeled flow path can be conservatively estimated. Microbial  $\text{SO}_4^{2-}$  reduction can be calculated by rearranging Eq. (12) (Table 5) to obtain Eq. (13) and applying the estimated rate of  $\text{SO}_4^{2-}$  reduction that was obtained for the sediment at site LA. Estimates of  $\text{FeS}_2$  oxidation were obtained by multiplying the calculated percentage of  $\text{SO}_4^{2-}$  derived from  $\text{FeS}_2$  oxidation in the flow-path segment (S95963 to S75034), which is assumed to be aerobic

(40–84%), and in the fourth segment (S47887 to S36803), which is anaerobic (19–34%), by the rates of  $\text{SO}_4^{2-}$  mass transfer. The estimate of  $\text{SO}_4^{2-}$  reduction was estimated along the aerobic part of the flow path (site LA) and along the anaerobic part (site MA) (Table 8). Under the assumption that  $\text{SO}_4^{2-}$  diffusing to groundwater is continuously utilized by  $\text{SO}_4^{2-}$ -reducing bacteria, the estimate for microbial  $\text{SO}_4^{2-}$  reduction can be converted to  $\text{CO}_2$  production ( $\text{CO}_2 \text{ SO}_4^{2-}$ ) by Eq. (14), where the “2” is the stoichiometric coefficient of  $\text{CO}_2$  in Eq. (4) (Table 9). Results indicate that ( $\text{CO}_2 \text{ SO}_4^{2-}$ ) (Table 9) is close to the estimated DIC mass transfer under anaerobic conditions (Table 6) and is consistent with the notion that  $\text{SO}_4^{2-}$  reduction is the dominant TEAP coupled to lignite oxidation in the anaerobic part of the flow path.

$\text{CO}_2$ -production rates also were calculated from estimated mass-transfer rates of  $\text{O}_2$  and  $\text{Fe(III)}$  for aerobic and anaerobic parts of the flow path (Table 9) with the stoichiometry shown in Eqs. (15) and (16).

Table 9

$\text{CO}_2$ -production rates in Magothy aquifer, Suffolk County, NY, as calculated from estimated  $\text{SO}_4^{2-}$ -reduction rates and from estimated mass-transfer rates for  $\text{SO}_4^{2-}$ ,  $\text{O}_2$ , and  $\text{Fe(II)}$  ( $\text{SO}_4^{2-}$ -reduction-rate calculations shown in Table 8)

Redox status of flow path segment	$\text{CO}_2$ production, calculated from $\text{CO}_2$ mass transfer ( $\text{mmol l}^{-1} \text{yr}^{-1} \times 10^{-4}$ )	$\text{CO}_2$ production, calculated from mass-transfer-rate estimates of electron acceptors ( $\text{mmol l}^{-1} \text{yr}^{-1} \times 10^{-4}$ )			
		$\text{CO}_{2(\text{O}_2)}$ production	$\text{CO}_{2(\text{Fe(II)})}$ production	$\text{CO}_{2(\text{SO}_4)}$ production	Total $\text{CO}_{2(x)}$ production
Aerobic	12.2–14.0	6.33–7.22	0	0.296–7.78	6.63–15
Anaerobic	3.57–4.07	0.0228–0.026	0.0198–0.0227	1.27–11.7	1.31–11.7

Estimates of SOM oxidized by O<sub>2</sub> in the aerobic zone (S95963 to S47887) are extremely high, as expected, and those in the anaerobic zone (S47887 to S36803) are low (Table 9). Estimates of SOM oxidized by Fe(III) (CO<sub>2</sub><sub>Fe(III)</sub>) may be underestimated by 1 or 2 orders of magnitude because Fe(II) is sequestered in sediments or reoxidized after Fe(III) reduction. Despite the uncertainty in these calculations, the total estimated CO<sub>2</sub> from organic matters that is oxidized by electron acceptors along the Magothy flow path is similar to CO<sub>2</sub> production rates obtained in DIC mass transfer calculations (Table 9). The smaller increase in SO<sub>4</sub><sup>2-</sup> concentration within the aerobic zone relative to the anaerobic zone (Fig. 3D) contradicts the somewhat constant rates of SO<sub>4</sub><sup>2-</sup> diffusion calculated for both parts (Table 8) and may result from the difficulty in comparing chemistry of pore water with chemistry of water from wells.

## 5. Conclusions

Estimated mass-transfer rates indicate that the principal electron-acceptors are O<sub>2</sub> and SO<sub>4</sub><sup>2-</sup> near the recharge area and SO<sub>4</sub><sup>2-</sup> in the anaerobic, distal parts of the flow path. Measured H<sub>2</sub> concentrations in groundwater confirm the predominance of SO<sub>4</sub><sup>2-</sup>-reducing TEAPs along the anaerobic part of the flow path and indicate a non-uniform distribution of SO<sub>4</sub><sup>2-</sup>- and Fe(III)-reducing zones in the Magothy. The predominance of SO<sub>4</sub><sup>2-</sup> reduction in the anaerobic part of the aquifer is supported by low concentrations of Fe(III) coatings on sediments, and the abundance of SO<sub>4</sub><sup>2-</sup> leached from poorly permeable sediments. The overall increase in SO<sub>4</sub><sup>2-</sup> concentrations, and the SO<sub>4</sub><sup>2-</sup> mass-transfer rates, along the flow path indicate that SO<sub>4</sub><sup>2-</sup> reduction is exceeded by the production of SO<sub>4</sub><sup>2-</sup> through diffusion from transitional-marine clays and by oxidation of FeS<sub>2</sub>. The δ<sup>34</sup>S of groundwater SO<sub>4</sub><sup>2-</sup> becomes "lighter" with depth at the recharge area through the oxidation of FeS<sub>2</sub>. Away from the recharge area, δ<sup>34</sup>S of water gradually becomes "heavier" as a result of: (1) mixing with "heavier" SO<sub>4</sub><sup>2-</sup> that originates from seawater anion complexes sorbed in poorly permeable sediments; and (2) SO<sub>4</sub><sup>2-</sup> reduction and the subsequent formation of FeS<sub>2</sub>. Fe(III) reduction is active locally in the Magothy

aquifer, and the high dissolved iron concentrations that result pose a costly problem for water suppliers.

Microenvironments can locally affect the concentrations of iron or other contaminants in coastal plain aquifers and may require detailed study of redox-active constituents, including O, Fe, S and C. For example, sulfate-reducing zones may yield water with low dissolved iron concentrations, and would, therefore, be suitable for water-supply development. The effects of localized microbial and geochemical processes can be vastly obscured by dilution and mixing by pumping, however, and water samples from wells are unlikely to reflect these processes. Therefore, detailed analysis of pore water and sediment geochemistry is needed in addition to ground-water sampling from wells to determine the effects of local microbial and geochemical reactions on ground-water.

## Acknowledgements

The Suffolk County Water Authority (SCWA) provided partial funding for this project. Gratitude is extended to Steven Colabufo, Richard Bova, Ed Rosovitch, Paul Kuzman and Robert Murray of SCWA for providing assistance with drilling, coring and supply-well sampling.

## References

- Appelo, C.A.J., Postma, D., 1993. *Geochemistry, Groundwater and Pollution*. Balkema, Rotterdam.
- Bennett, D.B., Taylor, M.A., Mulligan, J.F., Labiak, M., 1996. Impacts of water supply pumping on ground-water travel times in Nassau County, New York. Paper presented at American Institute of Hydrology, 1996 Annual Meeting, Boston, Massachusetts, 21–24 April.
- Blair, N., Leu, A., Munoz, E., Olsen, J., Kwong, E., des Marias, D., 1985. Anaerobic biodegradation of the lignin and polysaccharide components of lignocellulose and synthetic lignin by sediment microflora. *Applied and Environmental Microbiology* 47, 998–1004.
- Brown, C.J., 1998. Effects of geochemical and microbial reactions on iron and other redox-related constituents in the Magothy aquifer, Long Island, New York. PhD Thesis, State University of New York at Stony Brook, Stony Brook, New York.
- Brown, C.J., Coates, J.D., Schoonen, M.A.A., 1999. Localized sulfate-reducing zones in a coastal plain aquifer. *Ground Water* 37 (4), 505–516.
- Brown, C.J., Rakovan, J., Schoonen, M.A.A., 2000. Heavy minerals

- and organic carbon in Pleistocene and Cretaceous sediments on Long Island, with emphasis on pyrite and marcasite in the Magothy aquifer. US Geological Survey Water-Resources Investigations 99-4216, 22pp.
- Brown, E., Skougstad, M.W., Fishman, M.J., 1970. Methods for collection and analysis of water samples for dissolved minerals and gases. US Geological Survey Techniques of Water-Resources Investigations, Book 5, chap. A1, 160pp.
- Buxton, H.T., Modica, E., 1992. Patterns and rates of ground-water flow on Long Island, New York. *Ground Water* 30 (6), 857–866.
- Canfield, D.E., Raiswell, R., Bottrell, S., 1992. The reactivity of sedimentary iron minerals toward sulfide. *American Journal of Science* 292, 659–683.
- Carmody, R.W., Plummer, L.N., Busenberg, E., Coplen, T.B., 1998. Methods for collection of dissolved sulfate and sulfide and analysis of their sulfur isotope composition. US Geological Survey Open-File Report 97-234, 91pp.
- Chapelle, F.H., 1993. *Ground-water Microbiology and Geochemistry*. Wiley, New York.
- Chapelle, F.H., Lovley, D.R., 1990. Rates of microbial metabolism in deep coastal plain aquifers. *Applied Environmental Microbiology* 53 (11), 2636–2641.
- Chapelle, F.H., McMahon, P.B., 1991. Geochemistry of dissolved inorganic carbon in a coastal plain aquifer — 1. Sulfate from confining beds as an oxidant in microbial CO<sub>2</sub> production. *Journal of Hydrology* 127, 85–108.
- Chapelle, F.H., McMahon, P.B., Dubrovsky, N.M., Fujii, R.F., Oaksford, E.T., Vroblesky, D.A., 1995. Deducing the distribution of terminal electron-accepting processes in hydrologically diverse groundwater systems. *Water Resources Research* 31 (2), 359–371.
- Chapelle, F.H., Morris, J.T., McMahon, P.B., Zelibor, J.L., 1988. Bacterial metabolism and the  $\delta^{13}\text{C}$  composition of ground water, Floridan aquifer system, South Carolina. *Geology* 16, 117–121.
- Chapelle, F.H., Zelibor Jr., J.L., Grimes, D.J., Knobel, L.L., 1987. Bacteria in deep coastal plain sediments of Maryland—a possible source of CO<sub>2</sub> to ground water. *Water Resources Research* 23 (8), 1625–1632.
- Chukhrov, F.V., Zvyagin, B.B., Ermilova, L.P., Gorshkov, A.S., 1973. New data on iron oxides in the weathering zone. In: Serratos, J.M. (Ed.), *Proceedings of the International Clay Conference: Madrid, Spain, Division de Ciencias C.S.I.C.*, pp. 333–341.
- Coplen, T.B., 1993. Uses of environmental isotopes. In: Alley, W.M. (Ed.), *Regional Ground-Water Quality*, Van Nostrand Reinhold, New York, pp. 227–254.
- Cravotta III, C.A., 1998. Effect of sewage sludge on formation of acidic ground water at a reclaimed coal mine. *Ground Water* 36 (1), 9–20.
- Faust, G.T., 1963. Physical properties and mineralogy of selected samples of the sediments from the vicinity of the Brookhaven National Laboratory, Long Island, New York: US Geological Survey Bulletin 1156-B, 34.
- Fredrickson, J.K., Brockman, F.J., Workman, D.J., Li, S.W., Stevens, T.D., 1991. Isolation and characterization of a subsurface bacterium capable of growth on toluene, naphthalene, and other aromatic compounds. *Applied Environmental Microbiology* 57, 796–803.
- Hach Company, 1993. *DR/2000 Spectrophotometer Procedures Manual*. Hach Company, Loveland, CO, USA (450pp).
- Heron, G., Christensen, T.H., 1995. Impact of sediment-bound iron on redox buffering in a landfill leachate polluted aquifer (Vejen, Denmark). *Environmental Science and Technology* 29, 187–192.
- Heron, G., Crouzet, C., Bourg, A.C.M., Christensen, T.H., 1994a. Speciation of Fe(II) and Fe(III) in contaminated aquifer sediments using chemical extraction techniques. *Environmental Science and Technology* 28, 698–1705.
- Heron, G., Christensen, T.H., Tjell, J.C., 1994b. Oxidation capacity of aquifer sediments. *Environmental Science and Technology* 28, 153–158.
- Lonnice, T.P., 1982. Mineralogical and chemical comparison of marine, nonmarine, and transitional clay beds on south shore of Long Island, New York. *Journal of Sedimentary Petrology* 52 (2), 529–536.
- Lovley, D.R., 1987. Organic matter mineralization with the reduction of ferric iron — a review. *Geomicrobiology Journal* 5 (3/4), 375–399.
- Lovley, D.R., Chapelle, F.H., Phillips, E.J.P., 1990. Fe(III)-reducing bacteria in deeply buried sediments of the Atlantic Coastal Plain. *Geology* 18, 954–957.
- Lovley, D.R., Coates, J.D., Blunt-Harris, E.L., Phillips, E.J.P., Woodward, J.C., 1996. Humic substances as electron acceptors for microbial respiration. *Nature* 382, 445–448.
- Lovley, D.R., Goodwin, S., 1988. Hydrogen concentrations as an indicator of the predominant terminal electron-accepting reaction in aquatic sediments. *Geochimica Cosmochimica Acta* 52, 2993–3003.
- Lovley, D.R., Phillips, E.J.P., 1986a. Availability of ferric iron for microbial reduction in bottom sediments of the freshwater tidal Potomac River. *Applied and Environmental Microbiology* 52, 751–757.
- Lovley, D.R., Phillips, E.J.P., 1986b. Organic matter mineralization with the reduction of ferric iron in anaerobic sediments. *Applied Environmental Microbiology* 51, 683–689.
- Lovley, D.R., Phillips, E.J.P., 1987. Rapid assay for microbially reducible ferric iron in aquatic sediments. *Applied Environmental Microbiology* 53 (7), 1536–1540.
- Luszczynski, N.J., 1961. Filter-press method of extracting water samples for chloride analysis. US Geological Survey Water-Supply Paper 1544-A, 8pp.
- McClymonds, N.E., Franke, O.L., 1972. Water-transmitting properties of aquifers on Long Island, New York. US Geological Survey Professional Paper 627-E, 24pp.
- McKibben, M.A., Barnes, H.L., 1986. Oxidation of pyrite in low temperature acidic solutions—rate laws and surface textures. *Geochimica et Cosmochimica Acta* 50, 1509–1520.
- McMahon, P.B., Chapelle, F.H., 1991. Microbial production of organic acids in aquifer sediments and its role in aquifer geochemistry. *Nature* 349 (6306), 233–235.
- McMahon, P.B., Williams, D.F., Morris, J.T., 1990. Production and carbon isotopic composition of bacterial CO<sub>2</sub> in deep coastal

plain sediments of South Carolina. *Ground Water* 28 (5), 693-702.

Moses, C.O., Nordstrom, D.K., Herman, J.S., Mills, A.L., 1987. Aqueous pyrite oxidation by dissolved oxygen and ferric iron. *Geochimica et Cosmochimica Acta* 51, 1561-1571.

Murphy, E.M., Schramke, J.A., Fredrickson, J.K., Bledsoe, H.W., Francis, A.J., Sklarew, D.S., Linehan, J.C., 1992. The influence of microbial activity and sedimentary organic carbon on the isotope geochemistry of the Middendorf Aquifer. *Water Resources Research* 28 (3), 723-740.

Pearson Jr, F.J., Friedman, I., 1970. Sources of dissolved carbonate in an aquifer free of carbonate minerals. *Water Resources Research* 6 (6), 1775-1781.

Perlmutter, N.M., Geraghty, J.J., 1963. Geology and ground-water conditions in southern Nassau and southeastern Queens Counties, Long Island, N.Y. US Geological Survey Water-Supply Paper 1613-A, 205pp.

Plummer, L.N., 1988. Estimation of in situ rates of sulfate reduction in the Madison Limestone aquifer in parts of Wyoming, Montana, and South Dakota, by geochemical reaction modeling. *Eos* 69 (44), 1182.

Pucci Jr, A.A., Ehlke, T.A., Owens, J.P., 1992. Confining effects of ground-water quality in the New Jersey Coastal Plain. *Ground Water* 30 (3), 415-427.

Smolensky, D.A., Buxton, H.T., Shernoff, P.K., 1989. Hydrologic framework of Long Island, New York. US Geological Survey Hydrologic Investigations Atlas HA-709, 3 sheets, scale 1:250,000.

Taylor, B.E., Wheeler, M.C., Nordstrom, D.K., 1984. Isotopic composition of sulphate in acid mine drainage as measure of bacterial oxidation. *Nature* 308, 538-541 (Letters).

Trapp, H., Jr., Meisler, H., 1992. The regional aquifer system underlying the northern Atlantic Coastal Plain in parts of North Carolina, Virginia, Maryland, Delaware, New Jersey, and New York — summary. US Geological Survey Professional Paper 1404-A, 33pp.

Veizer, J., Jansen, S.L., 1985. Basement and sedimentary recycling — 2. Time Dimension to global tectonics. *The Journal of Geology* 93, 625-643.

Walter, D.A., 1997. Effects and distribution of iron-related well-screen encrustation and aquifer biofouling in Suffolk County, Long Island, New York. US Geological Survey Water-Resources Investigations Report 96-4217, 29pp.